

A MATHEMATICAL MODEL FOR ANALYSIS OF  
THE CELL CYCLE IN HUMAN TUMOUR

**Britta Basse, Bruce C. Baguley, Elaine S. Marshall,  
Wayne R. Joseph, Bruce van Brunt, Graeme Wake,  
and David J. N. Wall**

*Biomathematics Research Centre,  
Department of Mathematics & Statistics,  
University of Canterbury,  
Private Bag 4800, Christchurch, New Zealand.*

**Report Number:** UCDMS2002/8

August, 2002

**Keywords:** human tumour cells, flow cytometry, cell division cycle, steady state, exponential growth, paclitaxel



Britta Basse · Bruce C. Baguley · Elaine S. Marshall · Wayne R. Joseph · Bruce van Brunt · Graeme Wake · David J. N. Wall

## A Mathematical Model for Analysis of the Cell Cycle in Human Tumours

**Abstract.** The growth of human cancers is characterised by long and variable cell cycle times that are controlled by stochastic events prior to DNA replication and cell division. Treatment with radiotherapy or chemotherapy induces a complex chain of events involving reversible cell cycle arrest and cell death. In this paper we have developed a mathematical model that has the potential to describe the growth of human tumour cells and their responses to therapy. We have used the model to predict the response of cells to mitotic arrest, and have compared the results to experimental data using a human melanoma cell line exposed to the anticancer drug paclitaxel. Cells were analysed for DNA content at multiple time points by flow cytometry. An excellent correspondence was obtained between predicted and experimental data. We discuss possible extensions to the model to describe the behaviour of cell populations in vivo.

---

### 1. Introduction

The mammalian cell division cycle forms one of the cornerstones of our current understanding of tumour growth in humans and is dominated by four phases,  $G_1$ -phase,  $S$ -phase,  $G_2$ -phase and  $M$ -phase, with DNA replication occurring in  $S$ -phase and mitosis and cell division occurring in  $M$ -phase. The transitions from  $G_1$ -phase to  $S$ -phase, and from  $G_2$ -phase to  $M$ -phase, are controlled by all-or-nothing transitions involving a positive feedback system of cyclin-dependent kinases, cyclins and phosphatases ([16]). These transitions are the likely cause of the highly variable length of the cell cycle, most of which is accounted for by variability in  $G_1$ -phase duration ([22]). Early studies on cell cycle dynamics in cultured cells suggested the existence of a ‘transition probability’ regulating the commitment of  $G_1$ -phase cells to  $S$ -phase in order to account for this variability ([28]). In human cancers, the median cycle time also differs for individual cancer patients. The range of median cell cycle times varies from two days to several weeks with a median of approximately 6 days ([37]). Since the durations of  $S$ -phase,  $G_2$ -phase and  $M$ -phase are relatively short, most of the cancer cells in a patient’s tumour are in  $G_1$ -phase. Human cancer is characterised by a high rate of tumour cell turnover, such that the rate of cell death is up to 95% of the rate of cell division ([36]). Cell death may occur by two main processes, programmed death (apoptosis), which is likely to be the most common cause of cell turnover within a tumour, and necrosis, which is generally caused by localised failure of the tumour’s blood supply.

Many mathematical models describing the behaviour of cell populations have been developed over the last half century, including models differentiated by size ([5,27]).

---

Bruce Baguley, Elaine Marshall, Wayne Joseph: Cancer Society Research Centre, Faculty of Medicine and Health Sciences, University of Auckland, Private Bag 92019, Auckland, New Zealand.

Britta Basse, Graeme Wake, David Wall: Biomathematics Research Centre, University of Canterbury, Private Bag 4800, Christchurch, New Zealand.

Bruce van Brunt: Institute of Fundamental Sciences, Massey University, Private Bag 11 222, Palmerston North, New Zealand.

**Key words:** human tumour cells, flow cytometry, cell division cycle, steady state, exponential growth, paclitaxel

Variations of these models have been subject to rigorous mathematical analysis, especially in terms of the existence and stability of the steady size distribution that they may exhibit under certain conditions (see [8,9,15,31,12,25]). Cell size models have been reviewed by [2]. Other studies on cell cycle control have used an age structured approach ([26,32,23,19]) or modelled molecular events ([6]).

In this paper we have explored an alternative approach to the analysis of human cell cycle dynamics. We have used DNA content as a measure of the generic term ‘cell size’ in the model because the transitions from  $G_1$ -phase to  $S$ -phase and from  $M$ -phase to cell division are accompanied by changes in DNA content, which can be measured in a tumour population by flow cytometry. We have also included terms that have the potential to describe cell loss from a population. Since DNA content is measured in individual cells as they traverse a laser beam and inhomogeneity of illumination leads to a Poisson distribution of values, we have included a term to reflect the methodological aspects of flow cytometry. The mathematical model therefore provides a visual output that can be compared directly with experimental findings. As an initial step in the mathematical analysis of cell cycle perturbation, we have examined the effect of inhibition of cell division on the cell cycle distribution of a human melanoma cell line (NZM6). We have exposed this line to the drug paclitaxel, a clinically important anticancer drug that prevents cell division by arresting cells in mitosis ([24]), and have compared experimental data obtained using flow cytometry to the predicted values of the model.

## 2. Mathematical Model

For the mathematical model we chose four compartments representing the sub-populations of cells,  $G_1$ ,  $S$ ,  $G_2$ , and  $M$ , distinguished by their position within the cell cycle (Figure 1). The transition from  $G_2$ -phase to  $M$ -phase cannot easily be measured by flow cytometry, but we consider that it is an important part of the model. The dependent variables,  $G_1(x,t)$ ,  $S(x,t)$ ,  $G_2(x,t)$  and  $M(x,t)$ , can each be thought of as the number density of cells with relative DNA content  $x$  at time  $t$ . Directly after cell division, a newly divided daughter cell with relative DNA content scaled to  $x = 1$ , will double its DNA content during  $S$ -phase, so that at mitosis this model of the cell has relative DNA content approximately  $x = 2$ .

The movement between the four compartments is represented by the schematic diagram in Figure 1 which expresses the accumulation in each compartment and the movement between them. Our model equations are:

$$\frac{\partial G_1}{\partial t}(x,t) = 2^2 bM(2x,t) - (k_1 + \mu_{G_1})G_1(x,t), \quad (1)$$

$$\frac{\partial S}{\partial t}(x,t) = D \frac{\partial^2 S}{\partial x^2} - \mu_S S(x,t) - g \frac{\partial S}{\partial x}(x,t) + k_1 G_1(x,t) - I(x,t; T_S), \quad (2)$$

$$\frac{\partial G_2}{\partial t}(x,t) = I(x,t; T_S) - (k_2 + \mu_{G_2})G_2(x,t), \quad (3)$$

$$\frac{\partial M}{\partial t}(x,t) = k_2 G_2(x,t) - bM(x,t) - \mu_M M(x,t), \quad (4)$$

where the domain of definition is:  $0 < x < \infty$ , and  $t > 0$ . The time variable,  $t$ , is measured in hours while  $x$ , relative DNA content, is dimensionless. All parameters in the model may be functions of either  $t$  or  $x$  or both.

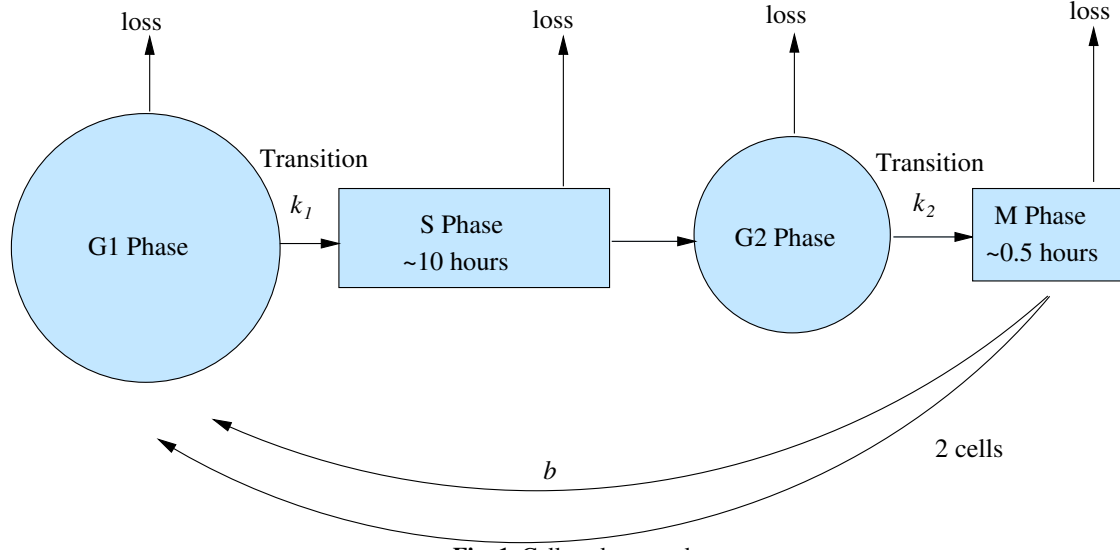


Fig. 1. Cell cycle control

In equation (1), describing  $G_1$ -phase, the first term on the right-hand-side is the source term provided by the influx of newly divided daughter cells from  $M$ -phase. A cell in  $M$ -phase divides into two identical daughter cells at a rate of  $b$  divisions per unit time. The  $2^2$  part of this term arises from the fact that, at division, all cells with DNA content in the interval  $[2x, 2x + 2\Delta x]$  are doubled in number and mapped to an interval with half the DNA content, namely  $[x, x + \Delta x]$ . Thorough derivations of similar non-local terms can be found in both [9] and [31]. The second term in equation (1) describes the loss of cells from  $G_1$ -phase due to either death (the  $\mu_{G_1} G_1(x, t)$  term) or transition to the  $S$ -phase ( $k_1 G_1(x, t)$ ). Therefore  $k_1$  provides the stochastic transition from the  $G_1$ -phase to  $S$ -phase and represents the probability per unit time per unit cell that the cell will enter the  $S$ -phase.

In equation (2), describing  $S$ -phase,  $g$  is the average rate at which the relative DNA content of a cell increases with time. For a homogeneous tumour cell population, cells in  $G_1$ -phase and  $G_2$  and  $M$ -phase, will each have constant DNA contents. However, in flow cytometry the cells are not all illuminated evenly as they pass through the flow cytometer and this causes an apparent variation of DNA content. The dispersion term,  $D \frac{\partial^2 S}{\partial x^2}$ , can be used to account for this variability. The inclusion of this parameter in the model allows us to compare model output DNA profiles directly with those obtained experimentally. Cells die in  $S$ -phase, equation (2), at a per capita rate of  $\mu_S$  per unit time. The term  $I(x, t; T_S)$ , given by equation (10) and discussed in section 2.1, represents the sub-population of cells which entered  $S$ -phase  $T_S$  hours previously and are ready to exit from  $S$ -phase to  $G_2$ -phase.

The loss term,  $I(x, t; T_S)$ , becomes the corresponding source term in the equation (3) representing  $G_2$ -phase. The second term in equation (3) accounts for the loss due to either exit to  $M$ -phase or cell death. Thus  $\mu_{G_2}$  is the per capita death rate of cells in  $G_2$ -phase while  $k_2$  is the transition rate of cells from  $G_2$ -phase to  $M$ -phase.

Finally in equation (4), we have cells dividing at a rate of  $b$  divisions per unit time. Cells die at the per capita rate of  $\mu_M$  per unit time and  $k_2 G_2(x, t)$  is the source term from  $G_2$ -phase. A summary of the model parameter descriptions and units is given in Table 1.

As it stands the model is incomplete as no side (initial or boundary) conditions have been specified for the equations (1)–(4); we rectify this now. In accordance with experimental evidence, we choose the following side data for these equations:

$$G_1(x,0) = \frac{a_0}{\sqrt{2\pi\theta_0^2}} \exp\left(-\frac{(x-1)^2}{2\theta_0^2}\right), \quad S(x,0) = 0, \quad 0 < x < \infty,$$

$$G_2(x,0) = 0, \quad M(x,0) = 0, \quad 0 < x < \infty,$$

$$D\frac{\partial S}{\partial x}(0,t) - gS(0,t) = 0, \quad t > 0.$$

The equation  $D\frac{\partial S}{\partial x}(0,t) - gS(0,t) = 0$  is a zero flux boundary condition. We choose the DNA content of cells in  $G_1$ -phase at time  $t = 0$  to be a Gaussian distribution with relative mean DNA content at  $x = 1$  and variance  $\theta_0^2$ . We choose  $\theta_0$  to be sufficiently small so that the extension of  $G_1(x,0)$  into the infeasible region  $x < 0$  is of no significance and we consider  $x > 0$  only. The variance,  $\theta_0$ , here reflects not only inter-cell heterogeneity of DNA content but also the observed DNA distribution (Poisson) seen in  $G_1$ -phase flow cytometry profiles which is a consequence of experimental error and the fact that cells are not illuminated evenly during flow cytometry. The total number of cells at time zero is

$$\int_0^\infty G_1(x,0) dx = \frac{a_0}{2} \left[ 1 + \operatorname{erf}\left(\frac{1}{\sqrt{2\theta_0}}\right) \right].$$

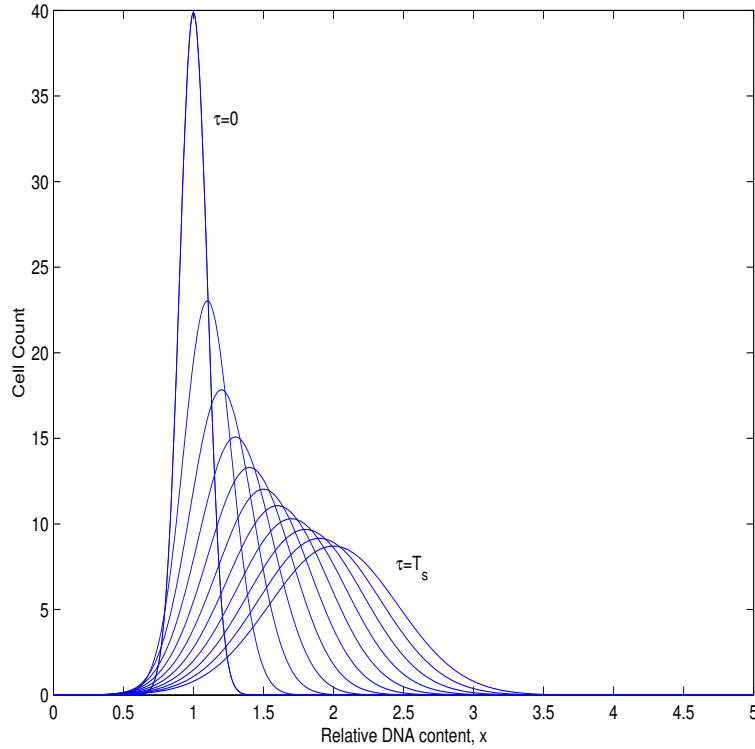


**Fig. 2.** The evolution of a distribution of cells,  $k_1G(x,t)$ , that enter  $S$ -phase from the  $G_1$ -phase at time  $\tau = 0$  hours. The incremental time step is 1 hour. The cell distribution labelled  $\tau = T_S = 10$  hours is about to be injected into the  $G_2$ -phase. The parameters are  $D = 0.01$ ,  $g = 0.1$ ,  $k_1 = 0.1$ ,  $\mu_S = 0$ , and  $G_1(x,t) = G_1(x,0) = \frac{a_0}{\sqrt{2\pi\theta_0^2}} \exp\left(-\frac{(x-1)^2}{2\theta_0^2}\right)$  where  $a_0 = 100$ ,  $\theta_0 = 0.1$ . For parameter descriptions and units see Table 1.

### 2.1. Examination of the cell transition from the S-phase

During S-phase (see equation (2)), the relative DNA content of a cell increases at an average rate  $g$  per unit time. The cells are modelled to leave the S-phase for the  $G_2$ -phase after a fixed time  $T_S$  hours. We now obtain an expression for this loss term,  $I(x, t; \tau = T_S)$ , of cells from S-phase to  $G_2$ -phase.

We denote the group of cells, entering S-phase at time  $t$  as  $I(x, t; \tau = 0) = I_0(x, t)$ . The model assumes that this group of cells simply enter S-phase, double their DNA content (or die) and then exit to the next phase ( $G_2$ ) without any interaction with cells that enter S-phase at different times. While in S-phase the DNA profile of the original cell cluster evolves dynamically as depicted in Figure 2. Thus, for a particular time  $t$ , the transition of the group of cells into S-phase occurs as an initial condition and the dynamics of any one particular cell group, while in S-phase, are governed by the homogeneous initial-boundary value problem:

$$\frac{\partial I}{\partial \tau}(x, t; \tau) + g \frac{\partial I}{\partial x} - D \frac{\partial^2 I}{\partial x^2} + \mu_S I = 0, \quad 0 < x < \infty, \quad t > \tau > 0, \quad (5)$$

with side conditions

$$I(x, t; \tau = 0) = I_0(x, t), \quad 0 < x < \infty, \quad t \geq 0, \quad D \frac{\partial I}{\partial x}(0, t) - gI(0, t) = 0, \quad t \geq \tau \geq 0. \quad (6)$$

Equation (5) is simply equation (2) with the source term,  $k_1 G_1(x, t)$ , and the loss term,  $I(x, t; T_S)$ , omitted.

By Laplace transformation techniques ([20], pp. 173), ([10], pp. 207 *et. seq.*), and the observation that the solution to the partial differential equation is translation invariant in the time variable, the solution to this associated equation is

$$I(x, t; \tau) = \begin{cases} \int_0^\infty I_0(y, t) \gamma(\tau, x, y) dy, & \tau, x, y > 0, \\ I_0(x, t), & \tau = 0, \end{cases} \quad (7)$$

where

$$\gamma(\tau, x, y) = \frac{e^{-\mu_S \tau}}{2\sqrt{\pi D \tau}} \left( e^{-((x-g\tau)-y)^2/4D\tau} - (1 + v(\tau, x, y)) e^{-((x+g\tau)+y)^2/4D\tau} \right), \quad \tau, x, y > 0 \quad (8)$$

with

$$v(\tau, x, y) = \frac{(x+y)}{g\tau} (1 + \mathcal{O}(\tau^{-1})).$$

Here  $\gamma$  is the Green's function for the partial differential operator in equation (5). It is seen that the formula for  $\gamma$  is valid for large time and this result follows from the Tauberian theorem for the Laplace transformation.

We now define

$$\tilde{I}(x, t; \tau) = \int_0^\infty I_0(y, t) \tilde{\gamma}(\tau, x, y) dy,$$

where

$$\tilde{\gamma} = \frac{e^{-\mu_S \tau}}{2\sqrt{\pi D \tau}} e^{-((x-g\tau)-y)^2/4D\tau},$$

it then follows that  $I = \tilde{I} - I_2$  where

$$I_2(x, t; \tau) = \int_0^\infty I_0(y, t) \tilde{\gamma}(\tau, x, y) (1 + v(\tau, x, y)) e^{-x(y+g\tau)/2D\tau} dy. \quad (9)$$

The kernel  $\tilde{\gamma}$  is the fundamental solution for the partial differential equation (5) when  $x \in (-\infty, \infty)$ ; *i.e.* when the second term in the parenthesis of equation (8) is not present. This second term is the image term and it ensures that the no-flux boundary condition is satisfied. For numerical evaluation of the  $I$  integral in our problem it is only necessary to use  $\tilde{I}$  as we show in the Appendix; this simplifies the analytical solution of equation (5) and is an acceptable approximation if the dispersion is small and  $I_0(x, t)$  is zero for small  $x$ .

At time  $t$ , the  $k_1 G(x, t - T_S)$  cells which entered  $S$ -phase  $T_S$  hours previously, are due to exit  $S$ -phase and enter  $G_2$ -phase. The loss term  $I(x, t; T_S)$  in equation (2) provides for this, and is obtained from equation (7) with the substitutions  $I_0(x, t) = k_1 G(x, t - T_S)$  and  $\tau = T_S$ , giving

$$I(x, t, T_S) = \begin{cases} \int_0^\infty k_1 G_1(y, t - T_S) \gamma(T_S, x, y) dy, & t \geq T_S, \\ 0 & t < T_S. \end{cases} \quad (10)$$

We observe that the transition term from the  $G_1$ -phase acts as a source term for the  $S$ -phase and note that both time variables,  $t$  and  $\tau$ , evolve at the same rate. Hence, by using Duhamel's principle ([17], pp. 70), we find that the number of cells in  $S$ -phase, and the solution of equation (2), is

$$S(x, t) = k_1 G(x, t) + \int_{0^+}^{t_1} \int_0^\infty k_1 G_1(y, t - \tau) \gamma(\tau, x, y) dy d\tau, \quad t_1 = \begin{cases} T_S, & t \geq T_S, \\ t, & t < T_S. \end{cases} \quad (11)$$

The distribution of cells in  $S$ -phase at a particular time  $t$  can be interpreted as an infinite sum of DNA profiles as depicted in Figure 2.

## 2.2. No dispersion in $S$ -phase:

By setting  $D = 0$  in equation (2), we obtain the case of no dispersion. Our side conditions remain unchanged except the boundary condition on  $x = 0$ ,  $S(0, t)$ , becomes the homogeneous Dirichlet condition. We again denote the transition of a group of cells from  $G_1$ -phase into  $S$ -phase as an initial condition,  $I(x, t; \tau = 0) = I_0(x, t)$ , where  $I(x, t; \tau)$  satisfies the equation

$$\frac{\partial I}{\partial \tau}(x, t; \tau) + g \frac{\partial I}{\partial x} + \mu_S I = 0, \quad 0 < x < \infty, \quad t > \tau > 0, \quad (12)$$

with side conditions

$$I(x, t; \tau = 0) = I_0(x, t), \quad 0 < x < \infty, \quad t \geq 0. \quad (13)$$

This gives

$$I(x, t; \tau) = \begin{cases} I_0(x - g\tau, t - \tau) e^{-\mu_S \tau}, & x > g\tau, \quad t > \tau \geq 0 \\ 0, & x \leq g\tau, \quad t > \tau \geq 0. \end{cases} \quad (14)$$

The term  $I(x, t; T_S)$  in equation (2), for the case of no dispersion ( $D = 0$ ), is then given by setting  $I_0(x, t) = k_1 G_1(x, t - T_S)$  and  $\tau = T_S$  in equation (14):

$$I(x, t; T_S) = \begin{cases} e^{-\mu_S T_S} k_1 G_1(x - gT_S, t - T_S), & x > gT_S, \quad t \geq T_S, \\ 0, & \forall x > 0, \quad t < T_S, \\ 0, & x \leq gT_S, \quad \forall t > 0. \end{cases} \quad (15)$$

Similarly the solution of equation (2) when  $D = 0$  is

$$S(x, t) = \int_0^{t_1} k_1 G_1(x - g\tau, t - \tau) e^{-\mu_S \tau} d\tau, \quad x > g\tau, \quad t_1 = \begin{cases} T_S, & t \geq T_S, \\ t, & t < T_S. \end{cases} \quad (16)$$

### 2.3. Steady DNA Distributions (SDD's) and model parameter values

In single functional equations and functional systems ([25]), it has been found that the dependent variables, in our case  $G_1(x, t)$ ,  $S(x, t)$ ,  $G_2(x, t)$  and  $M(x, t)$ , either grow or decay exponentially with time but their distribution in the  $x$ -variable is in steady state ([11–14, 35]). These are the type of distributions that we term steady DNA distributions (SDD's). The term asynchronous cell growth is also applied in the literature to describe SDD's ([1],[25],[23]). It has been shown ([25]) that this steady state in the  $x$ -variable is both uniquely determined by model parameters and is independent of the initial distribution at time  $t = 0$ .

SDD's are found experimentally via DNA profiles or histograms from flow cytometry and we simulate this type of temporal experimental data using our model (equations (1)-(4)). In an experiment we typically have a cell line with a steady DNA distribution. This cell line is then perturbed by either radiation or the addition of anticancer drugs. To model the resultant cell kinetics of the experiment we estimate a set of parameters for the model and then find the corresponding steady DNA distribution. The perturbed cell line is then modelled by altering model parameters. The main considerations are: How do we estimate the model parameters and which parameters should be altered to mimic the perturbed cell line kinetics. For the remainder of this subsection we discuss previously published results from a number of authors that help us gain preliminary estimates of model parameters for a cell population with a steady DNA distribution.

When a cell population has a steady DNA profile, the underlying system of equations are ordinary differential equations ([8]). Using this and the age structured modelling approach ([29, 33, 34]), it is possible to obtain estimates of model parameters of a cell population which has a steady DNA distribution. Equations (17) - (20) below give Steel's formulas ([29, 33]), for the average time spent in each phase as a function of the percentage of cells in each phase and the doubling time of the cell line.

$$T_c = T_d, \quad (17)$$

$$T_S = T_c \frac{\log\left(\frac{\%S + \%G_2M}{100} + 1\right)}{\log 2} - T_{G_2M}, \quad (18)$$

$$T_{G_2M} = T_c \frac{\log\left(\frac{\%G_2M}{100} + 1\right)}{\log 2}, \quad (19)$$

$$T_{G_1} = T_c - T_{G_2M} - T_S. \quad (20)$$

Here  $T_{G_1}$ ,  $T_S$  and  $T_{G_2M}$  are the average times spent in  $G_1$ ,  $S$ , and  $G_2M$  phase respectively.  $T_c$  is the cell cycle time and  $T_d$  is the doubling time of the cell population.  $\%G_1$ ,  $\%S$  and  $\%G_2M$  are the percentage of cells in  $G_1$ -phase,  $S$ -phase and  $G_2M$ -phase respectively. For a population of cells with a steady DNA distribution, the values of these percentages are unchanging in time.

We use the theory described by [30] which says that, for an SDD, the average time in each phase is related to the model parameters by the following equations:

$$T_{G_1} = \frac{1}{k_1 + \mu_{G_1}}, \quad (21)$$

$$T_S = \frac{1}{g + \mu_S}, \quad (22)$$

$$T_{G_2} = \frac{1}{k_2 + \mu_{G_2}}, \quad (23)$$

$$T_M = \frac{1}{b + \mu_M}. \quad (24)$$

The rate of convergence,  $R$ , to the SDD has been estimated by [7] as:

$$R = \frac{2\pi^2}{m} \left( \frac{CV_m}{m} \right)^2, \quad (25)$$

where  $m$  is the mean duration of the cell cycle and  $CV_m$  is the variation of the mean duration of the cell cycle. If we use  $m = T_c = T_{G_1} + T_S + T_{G_2} + T_M$ , we observe that if any of the denominators in equations (21)-(24) are close to zero, the length of time in that particular phase will tend towards infinity and the rate of convergence to the SDD will tend towards zero.

### 3. Results

#### 3.1. Flow cytometric studies

A human melanoma line (NZM6) was grown to a logarithmic phase of cell growth (exponential growth) using conditions that have been described previously ([18]). A mitotic inhibitor (paclitaxel) was then added at a concentration (200 nM) sufficient to inhibit cell division, and samples were removed for cell analysis at various times later. Flow cytometry was carried out by standard methods as described previously ([21]). A DNA standard (chicken red blood cells) was added to some of the samples to calibrate the cytometer.

#### 3.2. Model Results for NZM6

We used the model to mimic the cell kinetics of the human melanoma cell line NZM6 when the anticancer drug paclitaxel was added to this cell population at time  $t = 0$ . Prior to the addition of this drug, the cell line has a steady DNA distribution. We show that it is appropriate to use constant model parameter values to depict the dynamics of cell numbers as a function of DNA content and time. Since this cell line has minimal ability in steady state to undergo apoptosis, we denote the death rate parameters,  $\mu_{G_1}$ ,  $\mu_S$ ,  $\mu_{G_2}$ , and  $\mu_M$ , as zero.

For NZM6, the percentage of cells in each phase for cells with a steady DNA distribution was estimated by flow cytometric analysis as  $\%G_1 = 63.66$ ,  $\%S = 25.8$  and

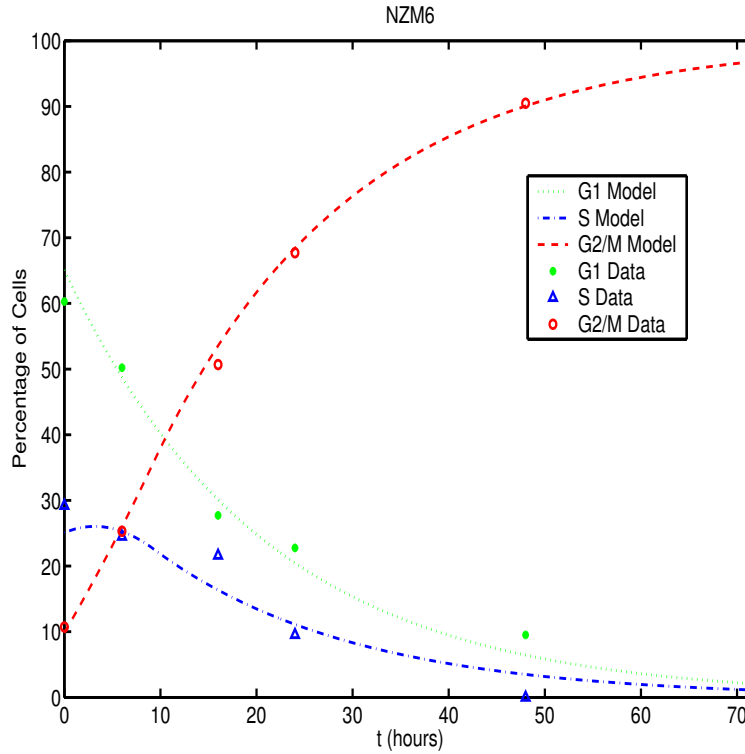


**Fig. 3.** Percentage of cells in each phase as a function of time. Model and Data for human cell line NZM6. Division stopped at  $t = 0$  hours. The DNA profiles at time  $t = 0$  and  $t = 72$  hours are given in Figures 4 and 5 respectively. Model parameters that were fitted were:  $k_1 = 0.0476$ ,  $g = 0.1129$ ,  $k_2 = 0.3193$  and  $b = 0.9296$ . The fixed parameters were dispersion  $D = 0.0001$ ; death rates  $\mu_{G_1} = \mu_S = \mu_{G_2} = \mu_M = 0$ ; starting distribution parameters  $a_0 = 100$ ,  $\theta_0 = 0.05$ ; mesh size  $\Delta t = 0.5$ ,  $\Delta x = 0.05$ ,  $t_{\max} = 100$ ,  $x_{\max} = 5$ . For parameter descriptions and units see Table 1.

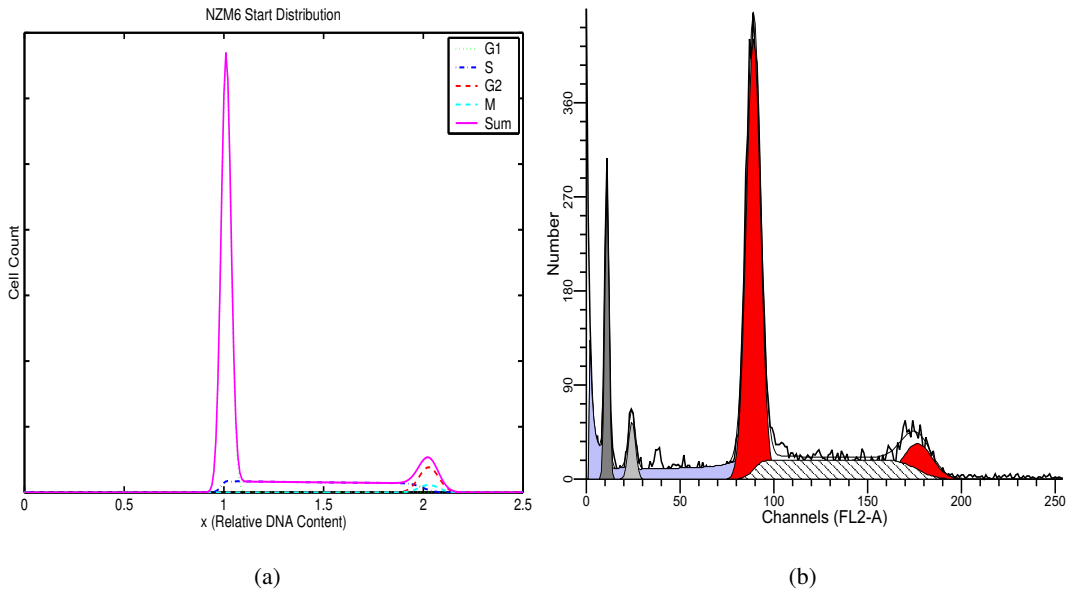


**Fig. 4.** Model (a) and experimental (b) steady DNA distribution (SDD) for human cell line NZM6 at time  $t = 0$ . Parameter values given in Figure 3. The shaded peaks in the left hand side of (b) indicate the internal standard for the flow cytometry.

$\%G_2M = 10.54$ . The doubling time for this cell line is approximately  $T_d = 29$  hours.

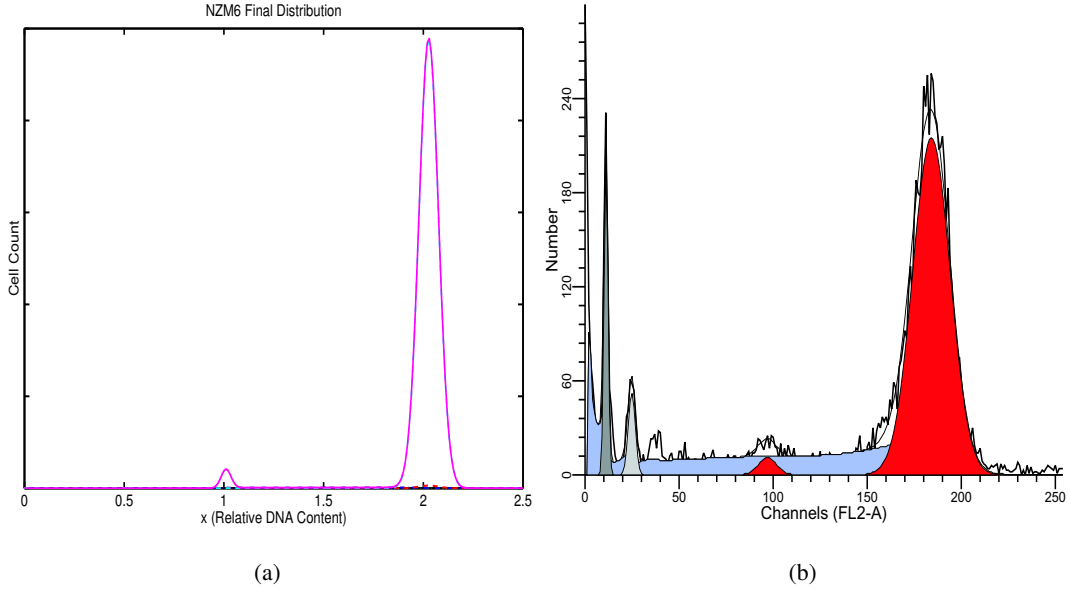


**Fig. 5.** Model (a) and experimental (b) DNA distribution (SDD) for human cell line NZM6 at time  $t = 72$  hours. The steady DNA distribution (SDD) was reached (see Figure 4) then division stopped ( $b = 0$ ) at time  $t = 0$  hours. It can be seen that cells have accumulated in the  $G_2M$ -phase region. Parameter values given in Figure 3. The shaded peaks in the left hand side of (b) indicate the internal standard for the flow cytometry.

Thus, substituting values of  $T_{G_1}$ ,  $T_S$ ,  $T_{G_2M}$ , and  $T_c$  from equations (17)-(20) into equations (21)-(24), and using the estimate of  $T_M = 0.5$  hours ([3]), we gain parameter estimates for the NZM6 cell line of;  $k_1 = 0.0624$ ,  $g = 0.1139$ ,  $k_2 = 0.8462$  and  $b = 2$ . The SDD associated with this parameter set was obtained by using the numerical method of finite differences to evaluate the model equations (1), (3) and (4). Simpsons's rule was used to estimate the integral in equation (11) for  $S$ -phase cells, with the substitution  $\tilde{\gamma}$  for  $\gamma$ .

To determine the existence of an SDD in the model, we measured the percentage of cells in  $G_1$ -phase at each time step and compared this to the percentage of cells in  $G_1$ -phase 5 hours previously. When the squared difference between these two values was less than 0.1%, we concluded that a SDD had been reached. To mimic the addition of paclitaxel and the simultaneous inhibition of cell division we set the division rate  $b$  to zero at time  $t = 0$  hours and ran the model for 72 hours. We calculated the percentage of cells in each phase as a function of time and compared this to the experimental data. We minimised the sum of squared errors in order to obtain model outputs as close as possible to the data. The sum of squared errors function is given by:

$$\mathcal{S}\mathcal{S}_{\text{NZM6}} = \sum_{j=1}^{\mathcal{J}} \sum_{i=1}^{\mathcal{I}} (P_i(t_j) - Y_i(t_j))^2, \quad (26)$$

where  $P_i(t_j)$  is the percentage of cells in phase number  $i$  at time  $t_j$  as predicted by the model and  $Y_i(t_j)$  is the corresponding data point. There are  $\mathcal{S} = 3$  phases found experimentally (being  $G_1$ ,  $S$  and  $G_2M$ -phase) and  $\mathcal{J}$  data points.

In this classic discrete inverse problem we wish to find a parameter estimation that minimises the sum of squared errors ([4]). The minimisation algorithm was supplied by the MATLAB function *fmincon*. This function uses a sequential programming method to

perform the optimisation procedure. The parameters we chose to fit were  $k_1$ ,  $g$ ,  $k_2$  and  $b$ . All other model parameters were fixed at the values specified in Figure 3. We imposed the constraints  $k_1 \in (0, 1]$ ,  $g \in (0.05, 2]$ ,  $k_2 \in (0, 1]$  and  $b \in (0, \infty]$ . These constraints ensure positivity of the parameter values, reflect the fact that  $k_1$  and  $k_2$  are probabilities and assume that the time spent in  $S$ -phase is approximately between 30 minutes and 20 hours. Figures 3, 4 and 5 indicate that the model describes accurate cell kinetics for melanoma cell line NZM6. It can be seen in Figure 3 that after the addition of paclitaxel, the percentage of cells in  $G_1$ -phase decline while those in  $G_2M$ -phase correspondingly increase. The percentage of cells in  $S$  phase decline after an initial time delay. We did not include the SDD data in our parameter fitting procedure but we see from comparisons with SDD data obtained experimentally (Figures 4 and 5) that our model gives similar DNA distributions. We found that the values  $k_1 = 0.0476$ ,  $g = 0.1129$ ,  $k_2 = 0.3193$  and  $b = 0.9296$  produce the least square error (117.85) between model and data as given by equation (26). The optimisation procedure was greatly assisted by first optimising with  $D = 0$  and then taking the result when  $D \neq 0$ . Such an optimisation procedure cannot be guaranteed of finding a global minimum of our objective function, equation (26). A sensitivity analysis of the value of this objective function to changes in parameter values indicates that our parameter estimation is unique in the feasible region of parameter space. It is also evident (Figure 6) that the objective function is not sensitive to changes in the division rate parameter close to the optimal value of  $b = 0.9296$ .

#### 4. Discussion

The model that we have developed represents an approach to the human tumour cell cycle that we consider has the potential to complement and extend previous models. We have modelled different phases of the cell cycle ([30,25,28]) and have validated the model using flow cytometry ([26,19,6,33]). We have also used results from an age modelling approach ([29,33]) to gain initial estimates of model parameters for a cell line with a steady DNA distribution. Our methodology differs from other models in that our measure of cell size ([5,27,8,9,31]) is cellular DNA content, we have included transition probabilities between phases and we have a dispersion term to allow for experimental variability in measurement of the DNA content so that we can directly compare model outputs with DNA profiles.

The transition probability terms linking  $G_1$ - to  $S$ -phase and  $G_2$ - to  $M$ -phase reflect the known variability in the length of the cell cycle. In contrast to this variability, the length of  $S$ -phase, which is accompanied by the progressive replication of DNA, is approximately constant and is of the order of 12 hours in human cancer cells. However, its length does vary among different human cancers ([37]) and it might therefore be expected to vary within a population. A dispersion term has therefore been provided to reflect this behaviour. The passage through  $M$ -phase, although it is considerably shorter than that for  $S$ -phase, similarly takes a finite time. An analogous term to that used for  $S$ -phase can be incorporated into the model to reflect this behaviour. This has been omitted from the current model because it plays only a very small role in modelling the behaviour of the NZM6 cell line.

We have shown that setting  $b$ , the division rate parameter for the NZM6 cell line, to zero was sufficient to model experimental results when paclitaxel was added to the cell population with steady DNA distribution. The success of the model in predicting

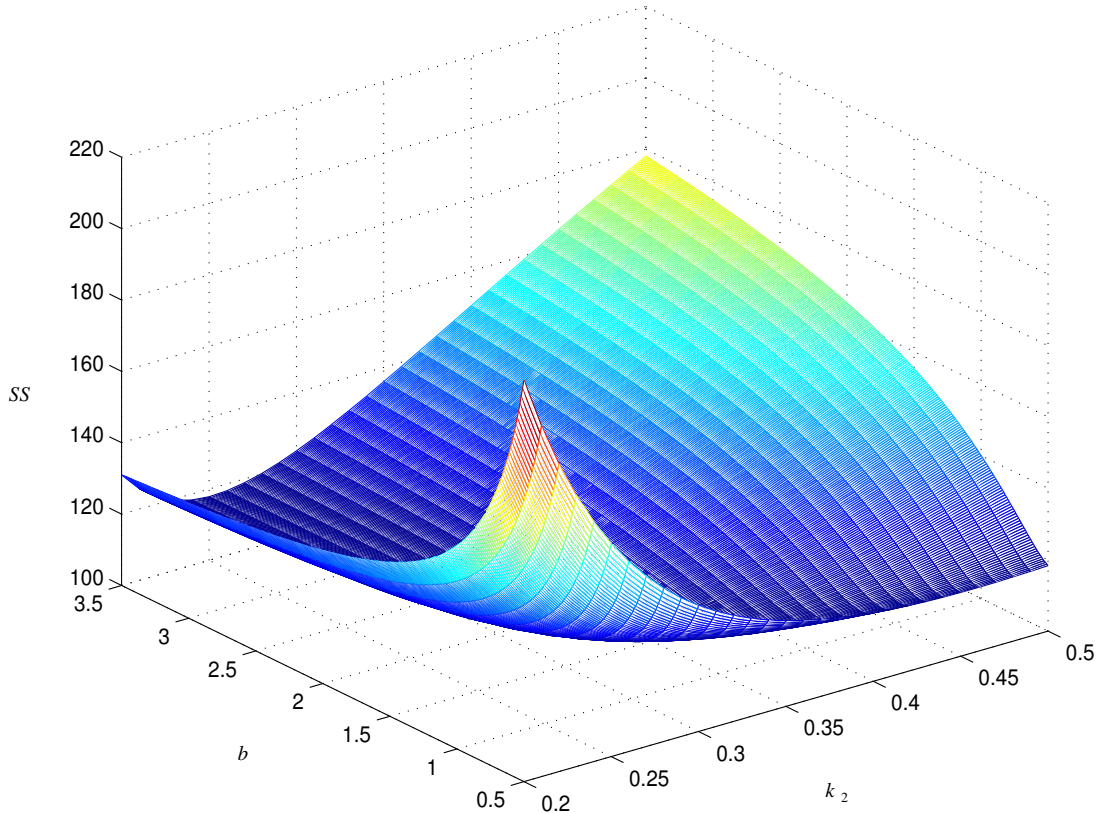


**Fig. 6.** The objective function (sum of squared errors), equation 26, as a function of the division rate,  $b$ , and  $k_2$ , the transition from  $G_2$  to  $M$ -phase. The minimum occurs at  $b = 0.9296$  and  $k_2 = 0.3193$  but the objective function value is not sensitive to larger values of  $b$  if  $k_2 = 0.3193$  is fixed. This can be seen in the plot as a valley that also bends in the  $k_2$  direction with  $b = 0.5$ . Other model parameter values are given in Figure 3.

the behaviour of these cells at different times after exposure to paclitaxel emphasises the value of the existing incorporated terms used to model the cycle phase transitions, and provides the background for extension to other human tumour cell lines. The nature of the terms in this model that link  $G_1$ - to  $S$ -phase and  $G_2$ - to  $M$ -phase will facilitate our understanding of the cell cycle, where all-or-nothing transitions are provided by positive feedback controls on the respective cdk2 and cdk1 enzyme complexes [18].

#### 4.1. Extension of the model to incorporate cell death, senescence and cycle arrest

Most human tumour cell lines growing in vitro under normal culture conditions have a low spontaneous death rate. However, exposure to agents such as radiation or chemotherapy can induce cell death, which generally occurs by apoptosis. Paclitaxel, used here to cause arrest of cell division, is thought to exert its anticancer effects by the induction of apoptosis subsequent to mitotic arrest ([24]). Apoptosis is accompanied by the progressive loss of cellular DNA, resulting in perturbation of the DNA flow cytometry profile. Our model can easily be extended to incorporate dying cells whose DNA content reduces progressively with time. This will facilitate the analysis of drug-treated populations where a proportion of cells is undergoing cell death and will also allow the description of the growth of human tumours in vivo. The model will include sub-population  $R(x, t)$  for this

removal phase, given by:

$$\begin{aligned} \frac{\partial R}{\partial t}(x,t) = D_R \frac{\partial^2 R}{\partial x^2}(x,t) + \frac{\partial(g_R R)}{\partial x}(x,t) \\ + (\mu_{G_1} G_1 + \mu_S S + \mu_{G_2} G_2 + \mu_M M), \quad 0 < x < \infty, \quad t > 0, \end{aligned} \quad (27)$$

with side conditions

$$R(x,0) = 0, \quad 0 < x < \infty, \quad D_R R(0,t) - g_R(0,t) = 0, \quad t \geq 0. \quad (28)$$

Equation (27) is virtually identical to equation (2), except cell DNA content is decreasing at an average rate  $g_R$  per unit time and the dispersion coefficient here is  $D_R$ . The source term in this equation is the sum of the loss (due to cell death) terms in equations (1)-(4).

Cell cultures treated with anticancer drugs or radiation may be induced to enter a senescent state during  $G_1$  phase. Again, the model can be modified to account for such behaviour by including a sub-population,  $G_0$  that will accumulate with time and can be written as

$$\frac{\partial G_0}{\partial t}(x,t) = -\mu_{G_0} G_0(x,t) + k_{G_0} G_1(x,t), \quad 0 < x < \infty, \quad t > 0, \quad (29)$$

with side conditions

$$G_0(x,0) = 0, \quad 0 < x < \infty, \quad (30)$$

where the term  $k_{G_0} G_1$  accounts for the transition rate into this senescent phase from the  $G_1$ -phase and  $\mu_{G_0}$  is the death rate in this phase. The term  $\mu_{G_0} G_0$  would join the source terms in the removal phase (equation (27)). The  $G_1$ -phase equation is accordingly modified to

$$\frac{\partial G_1}{\partial t}(x,t) = 2^2 b M(2x,t) - (k_1 + \mu_{G_1} + k_{G_0}) G_1(x,t), \quad (31)$$

with the other equations unmodified as per equations (2), (3) and (4).

A further response of cancer cells exposed to radiation or anticancer drugs is the induction of transient, reversible cell cycle arrest. Cycle arrest occurs most commonly by a change in rates of transition from  $G_1$ -phase to  $S$ -phase, and from  $G_2$ -phase and  $M$ -phase. These changes can be readily modelled by incorporating transient decreases in the corresponding equations for cell cycle transition.

The analysis of DNA profiles of cells obtained directly from human tumours are complex because of the presence of both tumour and normal cells. Moreover, two or more tumour cell populations with differing DNA content may be present, giving rise to multiple superimposed steady DNA distributions. Human cancer is also characterised by a high death rate ([36]) and by transitions of cells into a terminal non-growing or senescent state. Our model has the potential to model superimposed populations and to include terms for apoptosis, senescence and transient cell cycle arrest. These can be used to predict the effects of radiation and anticancer drugs, which are used for the treatment of human cancer. The profiles generated can be compared to experimental data from short-term culture of patients tumour material obtained at surgery. The ultimate aim of our approach is to provide insights as to why some patients fail to respond to treatment and to help in the development of strategies to overcome the resistance of their cancers to therapy.

## 5. Acknowledgements

This work was supported by grants from the Auckland Cancer Society, (B.C.B, E.S.M) and one of the authors (B.B) acknowledges the receipt of a University of Canterbury post doctoral scholarship.

### A. Appendix

The part of the integral in (7) corresponding to the image of  $\tilde{\gamma}$  in the boundary, namely  $I_2$ , when  $I_0(x, t) = 0$ ,  $x \leq \ell$ , where  $\ell$  is a positive real number, can be written as

$$I_2(x, t; \tau) = \int_{\ell}^{\infty} I_0(y, t) \tilde{\gamma}(\tau, x, y) (1 + v(\tau, x, y)) e^{-x(y+g\tau)/2D\tau} dy.$$

In this integral, when use is made of the positivity of both  $I_0$  and the exponential function, together with the mean value theorem for integrals, it is seen that

$$\begin{aligned} I_2 &= (1 + v(\tau, x, \xi)) e^{-x(\xi+g\tau)/2D\tau} \int_{\ell}^{\infty} I_0(y, t) \tilde{\gamma}(\tau, x, y) dy, \\ &\leq (1 + v(\tau, x, \xi)) e^{-x(\xi+g\tau)/2D\tau} \tilde{I}, \end{aligned}$$

where  $\xi \in (\ell, \infty)$ . It follows from this with  $\ell \approx 1$ ,  $x \approx 1$ ,  $\tau \leq 20$  and  $D$  as given in Table 1 that

$$I_2 \leq 2e^{-x(\ell+g\tau)/2D\tau} \tilde{I}.$$

Hence it follows for the parameter values used for this paper,  $I_2$  can be neglected with respect to  $\tilde{I}$  and the use of the approximate Green's function,  $\tilde{\gamma}$ , as is used in the numerical calculations has been justified.

## References

1. O. Arino, D. Axelrod, and M. Wuerz Kimmel, editors. *Mathematical Population Dynamics: Analysis of Heterogeneity*, volume 2: Carcinogenesis and Cell & Tumor Growth. Wuerz Publishing Ltd, Winnipeg, Canada, 1995.
2. O. Arino and E. Sanchez. A survey of cell population dynamics. *J. Theor. Med.*, 1:35–51, 1997.
3. B.C. Baguley, E.S. Marshall, and G.J. Finlay. Short-term cultures of clinical tumor material: potential contributions to oncology research. *Oncol. Res.*, 11:115–24, 1999.
4. J.V. Beck and K.J. Arnold. *Parameter estimation in engineering and science*. John Wiley, 1977.
5. G. Bell and E. Anderson. Cell growth and division. Mathematical model with applications to cell volume distributions in mammalian suspension cultures. *Biophys. J.*, 7:329–351, 1967.
6. G. Chiorini and M. Lupi. Variability in the timing of G1/S transition. *Math. Biosci.*, 2002. In press.
7. G. Chiorino, J.A.J. Metz, D. Tomasoni, and P. Ubezio. Desynchronization rate in cell populations: Mathematical modeling and experimental data. *J. Theor. Biol.*, 208:185–199, 2001.
8. O. Diekmann. Growth, fission and the stable size distribution. *J. Math. Biol.*, 18:135–148, 1983.
9. O. Diekmann, H. J. A. M Heijmans, and H. R. Thieme. On the stability of the cell size distribution. *J. Math. Biol.*, 19:227–248, 1984.
10. O. Föllinger. *Laplace und Fourier Transformation*. Hüthig Buch Verlag, Heidelberg, 1993.
11. A. J. Hall. *Steady Size Distributions in Cell Populations*. PhD thesis, Massey University, Palmerston North, New Zealand, 1991.
12. A. J. Hall and G. C. Wake. A functional differential equation arising in the modelling of cell-growth. *J. Aust. Math. Soc. Ser. B*, 30:424–435, 1989.
13. A. J. Hall and G. C. Wake. A functional differential equation determining steady size distributions for populations of cells growing exponentially. *J. Aust. Math. Soc. Ser. B*, 31:344–353, 1990.
14. A. J. Hall, G. C. Wake, and P. W. Gandar. Steady size distributions for cells in one dimensional plant tissues. *J. Math. Biol.*, 30(2):101–123, 1991.
15. K. B. Hannsgen and J. J. Tyson. Stability of the steady-state size distribution in a model of cell growth and division. *J. Math. Biol.*, 22:293–301, 1985.
16. I. Hoffmann and E. Karsenti. The role of cdc25 in checkpoints and feedback controls in the eukaryotic cell cycle. *J. Cell Sci. : Suppl.*, 18:75–79, 1994.

17. H. Kreiss and J. Lorenz. *Initial-Boundary Value Problems and the Navier-Stokes Equations*. Academic Press, San Diego, 1989.
18. E.S. Marshall, K.M. Holdaway, J.H.F. Shaw, G.J. Finlay, J.H.L. Matthews, and B.C. Baguley. Anticancer drug sensitivity profiles of new and established melanoma cell lines. *Oncol. Res.*, 5:301–309, 1993.
19. F. Montalenti, G. Sena, P. Cappella, and P. Ubezio. Simulating cancer-cell kinetics after drug treatment: Application to cisplatin on ovarian carcinoma. *Phys. Rev. E*, 57(5):5877–5887, May 1999.
20. A. Okubo. *Diffusion and Ecological Problems: Mathematical Models*. Springer-Verlag, Berlin, 1980.
21. J. Parmar, E.S. Marshall, G.A. Charters, K.M. Holdaway, and Baguley B.C. Shelling, A.N. Radiation-induced cell cycle delays and p53 status of early passage melanoma lines. *Oncol. Res.*, 12:149–55, 2000.
22. D.M. Prescott. Cell reproduction. *Int. Rev. Cytol.*, 100:93–128, 1987.
23. L. Priori and P. Ubezio. Mathematical modelling and computer simulation of cell synchrony. *Methods in cell science*, 18:83–91, June 1996.
24. W.C. Rose. Taxol - a review of its preclinical invivo antitumor activity. *Anticancer Drugs*, 3:311–321, 1992.
25. B. Rossa. *Asynchronous exponential growth in a size structured cell population with quiescent compartment*, chapter 14, pages 183–200. Volume 2: Carcinogenesis and Cell & Tumor Growth of Arino et al. [1], 1995.
26. G. Sena, C. Onado, P. Cappella, F. Montalenti, and P. Ubezio. Measuring the complexity of cell cycle arrest and killing of drugs: Kinetics of phase-specific effects induced by taxol. *Cytometry*, 37:113–124, 1999.
27. S. Sinko and W. Streifer. A new model for age-size structure of a population. *Ecology*, 48:330–335., 1967.
28. J.A. Smith and L. Martin. Do cells cycle? *Proc. Natl. Acad. Sci. U.S.A.*, 70:1263–1267, 1973.
29. G.G. Steel. *Growth kinetics of tumours*. Clarendon, Oxford, 1977.
30. M. Takahashi. Theoretical basis for cell cycle analysis. II. Further studies on labelled mitosis wave method. *J. Theor. Biol.*, 18:195–209, 1968.
31. J. J. Tyson and K. B. Hannsgen. Global asymptotic stability of the cell size distribution in probabilistic models of the cell cycle. *J. Math. Biol.*, pages 61–68, 1985.
32. P. Ubezio. Cell cycle simulation for flow cytometry. *Computer methods and programs in biomedicine. Section II. Systems and programs*, 31(3697):255–266, 1990.
33. P. Ubezio. Relationship between flow cytometric data and kinetic parameters. *Europ. J. Histochem.*, 37/supp. 4:15–28, 1993.
34. P. Ubezio, S. Filippeschi, and L. Spinelli. Method for kinetic analysis of drug-induced cell cycle perturbations. *Cytometry*, 12:119–126, 1991.
35. G. C. Wake, S. Cooper, H. K. Kim, and B. van Brunt. Functional differential equations for cell-growth models with dispersion. *Commun. Appl. Anal.*, 4:561–574, 2000.
36. J.V. Watson. Tumour growth dynamics. *Br. Med. Bull.*, 47:47–63, 1991.
37. G.D. Wilson, N.J. McNally, S. Dische, M.I. Saunders, C. Des Rochers, A.A. Lewis, and M.H. Bennett. Measurement of cell kinetics in human tumours in vivo using bromodeoxyuridine incorporation and flow cytometry. *Br. J. Cancer*, 58:423–431, 1988.

**Table 1.** Model parameters and variables

Parameter	Description	Dimensions	Value
$x$	relative DNA content	[1]	
$t$	time	hours	
$T_S$	time in $S$ -phase	hours	$\frac{1}{g}$
$G_1(x, t)$	number density of cells in $G_1$ -phase		
$S(x, t)$	number density of cells in $S$ -phase		
$G_2(x, t)$	number density of cells in $G_2$ -phase		
$M(x, t)$	number density of cells in $M$ -phase		
$D$	dispersion coefficient	$\frac{[x]^2}{[t]}$	0.0001
$g$	average growth rate of DNA in $S$ -phase	$\frac{[x]}{[t]}$	
$k_1$	transition probability of cells from $G_1$ to $S$ -phase	$\frac{1}{[t]}$	
$k_2$	transition probability of cells from $G_2$ to $M$ -phase	$\frac{1}{[t]}$	
$b$	division rate	$\frac{1}{[t]}$	
$\theta_0$	variance of starting distribution		0.05
$a_0$	height of starting distribution		100
$\mu_{G_1}$	death rate in $G_1$ -phase	$\frac{1}{[t]}$	
$\mu_S$	death rate in $S$ -phase	$\frac{1}{[t]}$	
$\mu_{G_2}$	death rate in $G_2$ -phase	$\frac{1}{[t]}$	
$\mu_M$	death rate in $M$ -phase	$\frac{1}{[t]}$	